Europe PMC Funders Group
Author Manuscript
ACS Nano. Author manuscript; available in PMC 2020 March 26.

Published in final edited form as:
ACS Nano. 2019 March 26; 13(3): 2936–2947. doi:10.1021/acsnano.8b07241.

Biomimetic Glyconanoparticle Vaccine for Cancer Immunotherapy

Eliran Moshe Reuven[#1], **Shani Leviatan Ben-Arye**[#1], **Hai Yu**[2], **Roberto Duchi**[3], **Andrea Perota**[3], **Sophie Conchon**[4], **Shirley Bachar Abramovitch**[1], **Jean-Paul Soulillou**[4], **Cesare Galli**[3,5], **Xi Chen**[2], **Vered Padler-Karavani**[1,*]

[1]Department of Cell Research and Immunology, Tel Aviv University, Tel Aviv, 69978, Israel

[2]Department of Chemistry, University of California-Davis, Davis, CA 95616, USA

[3]Avantea, Laboratory of Reproductive Technologies, Via Porcellasco 7/F, 26100 Cremona, Italy

[4]Institut de Transplantation–Urologie–Néphrologie, INSERM Unité Mixte de Recherche 1064, Centre Hospitalo Universitaire de Nantes, Nantes 44000, France

[5]FondazioneAvantea Cremona, Italy

[#] These authors contributed equally to this work.

Abstract

Cancer immunotherapy aims to harness the immune system to combat malignant processes. Transformed cells harbor diverse modifications that lead to formation of neoantigens, including aberrantly expressed cell surface carbohydrates. Targeting tumor-associated carbohydrate antigens (TACA) holds great potential for cancer immunotherapy. *N*-glycolylneuraminic acid (Neu5Gc) is a dietary non-human immunogenic carbohydrate that accumulates on human cancer cells, thereby generating neoantigens. In mice, passive immunotherapy with anti-Neu5Gc antibodies inhibits growth of Neu5Gc-positive tumors. Here we designed an active cancer vaccine immunotherapy strategy to target Neu5Gc-positive tumors. We generated biomimetic glyconanoparticles using engineered αGal knock-out porcine red blood cells to form nano-ghosts (NGs) that either express (NG^{pos}) or lack expression (NG^{neg}) of Neu5Gc-glycoconjugates in their natural context. We demonstrated that optimized immunization of 'human-like' Neu5Gc-deficient *Cmah*$^{-/-}$ mice with NG^{pos} glyconanoparticles induce a strong, diverse and persistent anti-Neu5Gc IgG immune response. Resulting anti-Neu5Gc IgG antibodies were also detected within Neu5Gc-positive tumors and inhibited tumor growth *in vivo*. Using detailed glycan microarray analysis, we further demonstrate that the kinetics and quality of the immune responses influence the efficacy of the

Corresponding Author: Department of Cell Research & Immunology, The George S. Wise Faculty of Life Sciences, Tel Aviv University, Tel Aviv 69978 Israel. Tel: +972-3-640-6737. Fax: +972-3-642-2046. vkaravani@tauex.tau.ac.il.

Author Contributions

V.P-K designed the experiments and supervised the project. E.M.R. and S.L.B-A performed the research; H.Y., R.D., A.P., S.C., J-P.S., C.G. and X.C. provided crucial reagents; S.B.A analyzed FACS of immune cells. E.M.R., S.L.B-A and V.P-K. wrote the paper, and all authors read and approved the manuscript. ‡These authors contributed equally.

Conflict of Interests

The authors declare no competing financial interest.

Europe PMC Funders Author Manuscripts
Europe PMC Funders Author Manuscripts

vaccine. These findings reinforce the potential of TACA neoantigens, and the dietary non-human sialic acid Neu5Gc in particular, as immunotherapy targets.

Keywords

neoantigen; cancer immunotherapy; biomimetic; glyconanoparticle; glycan microarray; sialic acid; *N*-glycolylneuraminic acid (Neu5Gc)

Immunotherapy for cancer treatment has made important advancement in recent years.[1, 2] It generally aims to induce or expand the host anti-cancer immune response that can distinguish subtle differences between cancer and normal cells.[3] The three common immunotherapies are: targeted cellular therapeutics (*i.e.* adoptive T cell therapy),[4–6] immune checkpoint blockade (*e.g.* blocking monoclonal antibodies targeting CTLA-4, PD-1 or PD-L1), [7–9] and therapeutic cancer vaccines.[10] Based on their composition, vaccines can stimulate adaptive immune responses of tumor-specific cytotoxic T cells and antibodies against tumorassociated antigens,[3, 11, 12] yet with only limited success,[3, 11, 13–15] mainly due to difficulties in identifying target antigens.[3]

Although carbohydrates have long been considered to be poorly immunogenic, their enormous potential as therapeutic targets led to design of carbohydrate-based vaccines.[16–19] Carbohydrate chains (glycans) are ubiquitously expressed on the surface of cells, where they are optimaly located for recognition by antibodies and immune receptors, either for protection or for elimination. Thus, various carbohydrate-based vaccines have been actively pursued to target not only various bacteria, viruses or parasites, but also cancer cells.[16, 17, 20] Cancer cells express aberrant glycosylation patterns compared to normal cells, and TACAs can be targeted for tumor cell killing through direct apoptosis, Fc-positive effector cells or complement.[21–23]

Sialic acids (Sia) cover cell surface glycans and frequently have altered expression on cancer cells that correlate with cancer progression and/or metastasis.[24–28] *N*-acetylneuraminic acid (Neu5Ac) and its hydroxylated form, *N*-glycolylneuraminic acid (Neu5Gc), are the two major Sia forms in mammals.[29] While humans cannot synthesize Neu5Gc due to a specific inactivation of the *CMAH* gene,[30] this non-human Sia incorporates into human cells through consumption of red meat and dairy,[31, 32] and substantially accumulate on carcinomas.[33] Thus, Neu5Gc presentation on tumor cells generates a variety of neoantigens that could potentially be targeted for immunotherapy. Passive transfer of anti-Neu5Gc antibodies inhibited growth of Neu5Gc-positive tumors *in vivo* in the human-like Neu5Gc-deficient *Cmah*$^{-/-}$ mouse model.[34, 35]

Here we investigated the potential targeting of Neu5Gc-neoantigens for immunotherapy by an active cancer vaccine. For this purpose, we generated biomimetic glyconanoparticles that express Neu5Gc-glycoconjugates in their natural context. As a control, we also generated equivalent glyconanoparticles that express Neu5Ac-glycoconjugates. Then, we optimized immunization of *Cmah*$^{-/-}$ mice with the cancer vaccine glyconanoparticles to induce a potent and sustained anti-Neu5Gc immune response, that inhibited tumor growth *in vivo*. Vaccine response was monitored by a robust high-throughput sialoglycan microarray, and

Europe PMC Funders Author Manuscripts

Europe PMC Funders Author Manuscripts

Europe PMC Funders Author Manuscripts

Europe PMC Funders Author Manuscripts

the analysis revealed that the kinetics and quality of the developed immune response influence the efficacy of the therapeutic cancer vaccine.

Results and Discussion

Generation and physical characterization of biomimetic glyconanoparticles

We designed an erythrocytes-based active cancer vaccine immunotherapy strategy to target Neu5Gc-positive tumors. Erythrocytes (red blood cells; RBCs) are attractive for various nano-biomedical applications.[36–38] RBCs are biconcave disc shaped cells (~7.8 μm × ~2.5 μm) that lack nucleus, with plasma membrane surface area of ~160 μm^2 (Figure 1A).[39, 40] RBCs are resistant to adhesion to endothelium, partly mediated by their glycocalyx that is abundantly covered with negatively charged sialic acids.[39, 41] To generate biomimetic glyconanoparticles that express Neu5Gc-TACA in their natural context, we used porcine-derived RBC that naturally express Neu5Gc-glycoconjugates due to their active CMAH enzyme. However, porcine also express the carbohydrate αGal (Galα1–3Galβ1–4GlcNAc-R) that is an immunogenic xenoantigen in humans, and against which all humans have circulating anti-Gal antibodies.[42] To eliminate the αGal antigen we used a porcine strain that is deficient in the *GGTA1* gene encoding the α1,3-galactosyltransferase (α1,3GT).[43] Thus, we used RBCs from two porcine knockout strains that express either Neu5Gc-glycoconjugates (Neu5Gc^{pos}; *Ggta*1$^{-/-}$ knocked-out strain;[43] Gal-KO), or control glycoconjugates that lack Neu5Gc, but instead express the non-immunogenic Neu5Ac (Neu5Gc^{neg}; double-knocked-out *Ggta*1$^{-/-}$/*Cmah*$^{-/-}$ strain;[44] Gal/Gc-DKO) (Figure 1a). RBCs were first purified from fresh blood of these porcine knockout strains by centrifugation and PBS wash. Then isolated RBCs went through membrane rupture in a hypotonic buffer to remove the intracellular contents. Next, the emptied RBC were washed, then re-suspended to form glycoproteolipid nano-ghost vesicles (NGs). These glyconanoparticles were designed to be biomimetic nano-sized particles containing a glycan shell that mediates its immunogenic properties.

We next examined the physiochemical properties of these NGs biomimetic glyconanoparticles using Cryo transmission electron microscopy (cryo-TEM), showing a similar and uniform morphology of NGs that either express Neu5Gc (Neu5Gc^{pos}–NG; NG^{pos}) or lack its expression (Neu5Gc^{neg}–NG; NG^{neg}) (Figure 1b). Dynamic light scattering (DLS) indicated that both NG^{pos}/NG^{neg} had a similar Zeta potential of approximately −25 mV (Figure 1c), and an average hydrodynamic diameter of ~400 nm (Figure 1d-e).

Further biochemical characterization demonstrated similar protein content by silver staining (Figure 2a), containing all expected major RBC membrane protein bands.[40] Subsequently, the sialic acid (Sia) content was compared between the two NGs preparations by Western blot developed with the Sia-binding proteins: lectins that binds both Neu5Ac- and Neu5Gc-that are Siaα2–6-linked to underlying glycans (*Sambucus Nigra Agglutinin*; SNA) or Siaα2–3-linked to underlying glycans (*Maackia Amurensis Lectin II*; MAL-II), and the polyclonal chicken-anti-Neu5Gc IgY that bind various Neu5Gc-containing glycans (Figure 2b).[45, 46] Sia-specific binding was confirmed by mild-periodate oxidation treatment that truncates two carbons off the Sia side chain, hence resulting in loss of Sia-binding.[47] This

Europe PMC Funders Author Manuscripts

Europe PMC Funders Author Manuscripts

biochemical analysis revealed that parallel glycoproteins bands were stained with both SNA and MAL-II lectins, demonstrating both terminal Siaα2–6 and Siaα2–3, and supporting a similar Sia content in both NG^{pos}/NG^{neg} (Figure 2b). Importantly, the Sia staining was mostly removed with periodate oxidation confirming Sia-specific recognition (Figure 2b). In addition, Neu5Gc was only present in NG^{pos} but not in NG^{neg}, and its staining was eliminated after treatment with periodate (Figure 2b). Taken together, these results indicate that the only difference between NG^{pos}/NG^{neg} preparations is the presence or lack of Neu5Gc expression, respectively. In fact, NG^{pos} contain diverse Neu5Gc-glycans, while NG^{neg} contain diverse Neu5Ac-glycans. Of note, the glycans on these two NGs preparations differ only by the additional hydroxyl group in glycans covered with Neu5Gc instead of Neu5Ac.

Surface Sia expression on NGs is critical for its application as a successful and reproducible active cancer vaccine. Once prepared, the NGs were kept frozen at −80 °C until further use. To monitor the stability of NGs after several freeze-thaw cycles, NGs were printed onto epoxide-activated glass slides using a nano-printer, then slides were developed with Sia-binding proteins. The results indicated that Sia content had not changed after one freeze-thaw cycle, however SNA and anti-Neu5Gc IgY reactivity had been greatly reduced at the second and third freeze-thaw cycles, respectively (Figure 2c). This is likely due to NGs degradation or inside-out flipping, both resulting in reduced expression of sialylated antigens. Similar results were obtained when freshly-prepared, or once-thawed NGs, were coated onto ELISA plate and examined with SNA, MAL-II and anti-Neu5Gc IgY, demonstrating stable reactivity after one freeze-thaw cycle (Figure 2d). Therefore, to preserve their efficacy all NGs preparations had been aliquoted and used fresh or after only one freeze-thaw cycle in all subsequent studies.

NGs vaccination allows sustained and robust anti-Neu5Gc antibody response

Active vaccination can induce a sustained and broad immune response, given optimization of various factors, such as antigen immunogenicity, adjuvant, number of exposures and intervals between exposures.[48, 49] To optimize the immunization protocol for sustained anti-Neu5Gc antibodies response in mice, we first immunized *Cmah*$^{-/-}$ mice with NG^{pos} (Neu5Gc-glycans) or control NG^{neg} (Neu5Ac-glycans) emulsified in Freund's Complete Adjuvant (FCA), followed by two boost injections emulsified in Freund's Incomplete Adjuvant (FIA), at two-week intervals (B2W; Figure S1a).

Mouse sera were collected weekly, then sera antibodies response was evaluated by sialoglycan microarrays printed with a diverse collection of Neu5Gc-glycans and Neu5Ac-glycans. This analysis showed an IgG response against only some of the Neu5Gc-glycans, which had dropped to baseline at week 6, two weeks after the second boost (Figure S1b-c). Adding a third boost at week 6 slightly improved the diversity of anti-Neu5Gc IgG response, that was also sustained through week 10 (B2W; Figure 3). In both immunization protocols (B2W, 2 or 3 boosts), there was a complete absence of response against any of the Neu5Ac-glycans, that differ by only a single oxygen atom from their counterpart Neu5Gc-glycans (Figure S1, Figure 3). Similarly, immunization with the control NG^{neg} (Neu5Ac-glycans) did not show any response against both Neu5Ac/Neu5Gc-glycans (Figure 3). These results

Europe PMC Funders Author Manuscripts

Europe PMC Funders Author Manuscripts

exemplify the tolerance against the native Neu5Ac-glycans, in contrast to the high immunogenicity of Neu5Gc-glycans.

Adjuvants can enhance and shape vaccine immune responses, and vaccine schedules can dramatically affect antibody magnitude and persistence, with longer intervals between injections generally yielding greater responses.[48] To evaluate the contribution of the adjuvant to the developed response in mice, *Cmah*$^{-/-}$ mice were immunized (B2W, 2 boosts) with NG^{pos} or NG^{neg}, with or without adjuvant. Analysis of sera obtained at week 6 revealed a clear contribution of the adjuvant to the level and diversity of the developed anti-Neu5Gc IgG response (Figure S2). Next, the interval between boost injections was further optimized and persistence of response evaluated. *Cmah*$^{-/-}$ mice were immunized with NG^{pos} in FCA, then with two boost injections in FIA after one and two weeks, followed by a third boost 6 weeks after primary immunization (B1W; Figure 3a). Glycan microarray analysis revealed a highly diverse, robust and persistent anti-Neu5Gc IgG response, that remained high even 10 weeks post primary immunization (Figure 3b). Boosting with the Neu5Gc-deficient NG^{neg}-FIA after primary immunization (Figure S3a) showed a much lower anti-Neu5Gc response compared to boosting with NG^{pos}-FIA (Figure S3b), while this change had no effect on the developed immune response against the NG-carrier, that was similar between the two boosting regimens (Figure S3c). Hence the presence of Neu5Gc during boosting is important for the development of anti-Neu5Gc response. Overall, the B1W vaccination regimen (weeks 0, 1, 2, 6) with NG^{pos} boosting, had proved to be more efficient than B2W (weeks 0, 2, 4, 6), yielding a high and specific anti-Neu5Gc IgG response that was sustained for at least 4 weeks after the third boost.

Evaluating cancer vaccine efficacy against Neu5Gc-positive tumors

Previous studies showed that treatment of Neu5Gc-positive tumors with passively transferred human[34] or mouse[35] anti-Neu5Gc antibodies in the Neu5Gc-deficient *Cmah*$^{-/-}$ mouse model have dualistic and contrasting responses.[34, 50, 51] While high dose anti-Neu5Gc antibodies inhibited tumor growth,[34] a low dose treatment actually promoted tumor growth.[34, 52, 53] Furthermore, the shift between these opposite dosage effects occurred at a very narrow range, of even only two-fold changes.[35] As such, anti-Neu5Gc antibodies are both cancer biomarkers and potential therapeutics.[34, 54]

To evaluate the active vaccination at a low quality of response, mice were immunized with NG^{pos} or NG^{neg} at the non-optimal B2W regimen (weeks 0, 2, 4; Figure S4a), then syngeneic Neu5Gc-positive tumors (mouse adenocarcinoma MC-38) were inoculated subcutaneously at week 5.5 and tumor growth monitored. While NG^{pos}-vaccinated mice showed a slight decrease in tumor growth compared to NG^{neg}-vaccinated group, this trend was not statistically significant (Figure S4b). Nevertheless, it was encouraging to find that, unlike passive therapy,[34, 35] even at a low quality of anti-Neu5Gc antibodies response (Figure S1), active vaccination did not mediate promotion of tumor growth, suggesting that the active vaccine is safe with respect to the negative low dose effects.

Next, we evaluated the therapeutic efficacy of the optimized active vaccine regimen and its effect on tumor growth *in vivo*. Mice were immunized with NG^{pos} or NG^{neg} at the optimal B1W regimen (weeks 0, 1, 2, 6), syngeneic Neu5Gc-positive MC-38 tumor cells were

Europe PMC Funders Author Manuscripts

inoculated subcutaneously at week 7.5 then tumor growth and antibodies responses monitored (Figure 4a). In this case, tumor growth was dramatically inhibited in the vaccine-treated group (NG^{pos}) compared to the control-treated group (NG^{neg}) (Figure 4b). All groups showed minimal serum IgM/IgG responses against the NG^{neg}-carrier, but higher response against NG^{pos}-carrier that is likely mediated by its immunogenic Neu5Gc component (Figure S5). Detailed glycan microarray analysis revealed that following NG^{pos} vaccination, exposure to the inoculated Neu5Gc-positive tumors at week 7.5 mediated a dramatic enhancement in the average anti-Neu5Gc IgG response, compared to the group that had not been exposed to the tumors (Figure 4c). This reflected an increase in antibodies binding reactivity against all examined Neu5Gc-glycans (Figure 4d), likely also representing an increase in the affinities of these antibodies.[55] In contrast, the inoculated tumors had no effect on the developed anti-Neu5Gc IgMs response (Figure S6) that had dramatically increased immediately after the third boost on week 6, even before tumor inoculation, then remained static for two weeks (Figure S6b). Importantly, the control NG^{neg} treatment did not result in any serum response against Neu5Gc-glycans, even after tumors inoculation (Figure 4c-d).

In humans when tumors develop later in life, the continued consumption of dietary Neu5Gc (red meat, dairy) result in its preferential accumulation on developed tumor cells,[32] due to their higher metabolism and elevated expression of Sialin, a sialic acid transporter.[56] Therefore, anti-Neu5Gc antibodies boosted response by Neu5Gc-positive tumors is likely to occur also in humans. In fact, it had been shown that some anti-Neu5Gc antibodies are elevated in carcinoma patients and can be used as cancer biomarkers.[34, 54]

Characterization of purified intra-tumoral IgG

Anti-Neu5Gc antibodies developed during the cancer vaccine treatment clearly play an important role in its therapeutic efficacy (Figure 4). One of the ways antibodies mediate tumor growth inhibition and/or killing, is by directly binding to their target antigens expressed on the surface of tumor cells.[57, 58] While NG^{pos} vaccine-treated mice showed tumor anti-Neu5Gc IgG boosting effect on weeks 8-9, noticeably, they also displayed a transient depletion of serum anti-Neu5Gc IgG on week 10 (2.5 weeks after tumor inoculation), that was not observed in the vaccine-treated group without inoculation of tumors (Figure 4c). The drop in average response reflected a similar trend in the response to almost all individual Neu5Gc-glycans (Figure 4d). To evaluate the hypothesis that these antibodies had migrated to the tumors, tumors were harvested, minced into suspension, then intra-tumoral antibodies were purified by protein-A to capture IgG antibodies. Glycan microarray analysis of purified intra-tumoral IgGs revealed that all vaccine-treated mice (NG^{pos}) had a strong and highly-specific binding reactivity against all Neu5Gc-glycans but not Neu5Ac-glycans (Figure 5a-b), supporting migration of serum anti-Neu5Gc IgGs into the growing tumor mass. On the other hand, antibodies purified from tumors of control vaccination (NG^{neg}; n=10) showed mostly very low reactivity on the arrays (Figure 5a-b). Interestingly, few mice in this control group had a very low but specific anti-Neu5Gc IgG response, likely mediated by the tumors that present foreign Neu5Gc-neoantigens. Notably, although MC-38 tumor cells express more Siaα2–3-linked than Siaα2–6-linked sialic acids,[35] no notable difference was detected in the epitopes recognized by the purified intra-

Europe PMC Funders Author Manuscripts

Europe PMC Funders Author Manuscripts

tumoral IgG. Both vaccine and control treated mice showed similar infiltration of immune cells ($CD45^+$ and $CD45^+CD3^+$; Figure S7). Altogether, these results suggest that anti-Neu5Gc IgG antibodies reach the tumor mass to mediate inhibition of tumor growth.

Evaluating heterogeneity in vaccine treatment

A key feature of vaccine therapy is the heterogeneity in the developed immune responses of different individuals to a given vaccine, in both the magnitude and decay rate of responses, as well as of a given individual to different vaccines.[59, 60] In cancer vaccine technology, tumor heterogeneity adds another level of complexity.[61] To evaluate heterogeneity in NG^{pos} vaccination treatment, the kinetics of anti-Neu5Gc IgG responses and tumor growth were monitored in each mouse individually (Figure S8). This analysis revealed three types of responses (Figure S8; Figure 6). Group 1 showed a late onset of response around week 6-7, with intermediate magnitude of response, and a low therapeutic effect on tumor. Group 2 showed a two-phase response initiating around weeks 3-4, followed by a secondary response immediately after the third boost vaccination on week 6, that had gradually decayed, with no therapeutic effect on tumors. By contrast, Group 3 showed a dramatic tumor inhibiting therapeutic effect, with a distinct pattern of antibodies kinetics. In this group, there was a two-phase response as in group 2, however in addition there was an almost complete depletion of anti-Neu5Gc IgG from the serum on week 10, that was restored a few days later by week 10.5 (Figure S8; Figure 6). Furthermore, only in group 3 the IgG titer seemed to be higher than the IgM (Figure S8d). This analysis clearly demonstrated that certain immune response kinetics, as developed in group 3, are more constructive in supporting the therapeutic effects mediated by the cancer vaccine.

Conclusions

While envisioned already in 1891,[62] only few cancer vaccines have been approved by the US Food and Drug Administration (FDA) thus far.[13, 61] The key barriers to their success are low antigenicity of targeting antigens, tumor heterogeneity,[61] and low mutational burden with only few peptide neoantigens in some cancers.[63] These limitations prompted the continued search for other potential antigens for vaccines.[64] Tumor-associated glycosylation changes generate carbohydrate-neoantigens that are excellent candidate targets for immunotherapy.[28, 65] In particular, Neu5Gc, the antigenic non-human dietary carbohydrate that accumulates on human carcinoma,[66, 67] generates a whole array of cancer neoantigens.[34,35]

Red blood cells have been investigated over 40 years as potential antigen delivery systems,[68–70] with some success in human patients,[71] and more recently as drug delivery vehicles,[72] including in nano-structured biomedical systems.[36–38] Here we designed an active cancer vaccine targeting Neu5Gc-TACAs in a mouse model, as a proof of concept. Taking advantage of RBCs biocompatibility and expected prolonged circulation time,[37, 39, 73] glyconanoparticles were prepared from engineered porcine erythrocytes membranes. These biomimetics were used to actively vaccinate ‘human-like’ Neu5Gc-deficient mice, after optimization of adjuvant and immunization schedules. The engineered NGs were designed to operate as a cancer vaccine to mount an effective immune response against cancer and

Europe PMC Funders Author Manuscripts

Europe PMC Funders Author Manuscripts

therefore were not expected to reach the tumor mass in order to facilitate killing. Taking advantage of the glycan microarrays technology for biomedical antibody profiling,[45, 65, 74–76] full analysis of responses against 48 different sialoglycans revealed a highly specific, robust and prolonged anti-Neu5Gc IgGs, with distinctive patterns of humoral responses in individual mice. Neu5Gc-positive tumors further enhanced the vaccine-developed humoral anti-Neu5Gc responses, as also expected in humans,[34] and the vaccine treatment inhibited tumor growth. Interestingly, 37.5% of mice optimally responded to the vaccine therapy, and revealed a specific pattern of antibodies response kinetics, that included their complete, but transient, depletion from circulation. This important kinetic feature can contribute to understanding the heterogeneity of responses to vaccines, and assist in prediction of responses.[77] While current investigation was focused on the antibodies responses, it is likely that the cellular arm of the immune system also participates in the successful therapeutic effects,[78–80] which would warrant cellular immune profiling in the future.

Methods

Materials

Dulbecco's Modified Eagle's Medium high Glucose (DMEM), Fetal Bovine Serum (FCS), L-Glutamine, Penicillin-streptomycin (pen-strep) Dulbecco's PBS were all purchased from biological industries; Trizma-hydrochloride, Tween-20, Ovalbumin (Grade V), Ophenylenediamine (OPD) and periodate were all purchased from Sigma-Aldrich, EDTA was purchased from Fisher Scientifics, Hydrogen peroxide 30% was purchased from Merck.

Antibodies and Lectins

Chicken anti-Neu5Gc IgY (Biolegend), biotinylated-SNA, biotinylated-MALII (Vector Lab). HRP-donkey-anti-chicken IgY, HRP-Streptavidin, Cy3-goat-anti–mouse IgG, Cy3-donkey-anti-chicken IgY and Cy3-Strepavidin (Jackson ImmunoResearch) were all from commercial sources.

Cell lines and Mice

MC38-GFP cells (murine colon adenocarcinoma cells stably expressing GFP,[81] kindly provided by Prof. Ajit Varki) were grown in culture (DMEM with high glucose, 10% FCS, 1% Glutamine, 1% penn-strep). *Cmah*$^{-/-}$ mice were bred and maintained according to Animal Care and Use Committee protocol approved by Tel Aviv University.

Generation of nano-ghost (NG) glyconanoparticles from porcine red blood cells

Nano-ghost glyconanoparticles (NG) were prepared from porcine red blood cells (RBC) of two strains: α-Gal *Ggta*1$^{-/-}$ knocked-out[43] and the double-KO *Ggta*1$^{-/-}$/*Cmah*$^{-/-}$ [44] (Gal/Gc-DKO; Neu5Gc-Negative; NG^{neg}) strains. RBC were packed by 3 rounds of centrifugation in PBS pH 7.4 (1000 × g, 10 min), and then stored at −80 °C until further use. Packed RBCs (2.5 ml) were lysed by incubation on ice with 25 ml of ice cold lysis buffer (50 mM of Tris-HCl, pH 7.35 containing 10 mM of EDTA) for 10 min, then centrifuged for 30 min at 26,000 × g with no brakes (to avoid pellet detachment). The supernatant was removed and the lysis procedure was repeated until NGs pellet became white. NGs pellet

Europe PMC Funders Author Manuscripts

Europe PMC Funders Author Manuscripts

was washed with 25 ml of ice-cold double distilled H_2O (DDW), then re-suspended in 1 ml DDW. Protein content was determined by BCA (Pierce), the volume was adjusted to a final concentration of 2 mg/ml, and then 1 ml aliquots were stored at −80 °C until further use. For physical characterization, NGs were stored at 4 °C and analyzed within 24 hours of preparation.

Cryo transmission electron microscopy (cryo-TEM)

NGs were diluted to 0.1 mg/ml and aliquots of 5 μl each were pipetted onto a plasma-etched (25 s) 200 mesh holey carbon grid (PELCO) held in the plunge chamber at approximate 90% humidity. Sample preparation was carried out using a Cryo-Plunge 3 unit (Gatan Instruments) employing a double blot technique. The samples were blotted for 2 s, and then plunged into liquid ethane at a temperature of −170 °C. After vitrification, the grids were transferred under liquid nitrogen to the cryo-TEM specimen holder (Gatan 626 cryo holder) at −170 °C. Imaging was carried out using a Tecnai G2 cryo-TEM (FEI Company, Eindhoven, Netherlands) operated at 120 kV with a Gatan 4000 camera, and images were captured using a Digital Micrograph software (Gatan). During imaging, the temperature of the sample holder was maintained at −170 °C to minimize sublimation of vitreous water.

Dynamic light scattering (DLS) to determine size and zeta potential

Freshly prepared NGs were diluted in PBS pH 7.4 (for size) or water (for zeta potential) to 20 μg/ml total protein and measured in a Malvern Nano ZS zetasizer. Data calculations were performed using the Zetasizer software with the Intensity algorithm. Each experimental result is an average of at least three independent measurements. Error bars represented mean ± SD, with size SD calculated by multiplying the Mean Size with square root of the PDI (Poly dispersity index).

Protein analysis of NGs by Silver staining

Freshly prepared NGs were diluted in SDS sample buffer to 40 ng/μl, incubated at room temperature (RT) for 30 min, then separated on 12% SDS-PAGE gels. Gels were fixed for 20 min at RT in 25 ml of fixation solution 1 (10% acetic acid, 40% ethanol, 50% DDW, 0.0185% Formaldehyde), then washed 3 times with 50% ethanol for 10 min each, sensitized for 1 min with 25 ml of 0.02% $Na_2S_2O_3$ in DDW, washed with water for 20 sec 3 times, then incubated for 12 minutes with 25 ml of Silver Nitrate solution (9.4 mM AgNO containing 0.02% formaldehyde), and washed 3 times with water for 20 sec each. Gels were developed using a Developing Solution (0.0005% $Na_2S_2O_3$, 0.015% formaldehyde, 5% Na_2CO_3) until bands appeared, then stopped with fixation solution 2 (10% acetic acid, 40% ethanol, 50% DDW), and gels were scanned.

Sialic acid content analysis of NGs by Western blotting

Sialic acid content was evaluated by lectin analysis of Western blots. Freshly prepared NGs were diluted in SDS sample buffer to 40 ng/μl, incubated at room temperature for 30 min, then separated on 12% SDS-PAGE gels, followed by transfer onto nitrocellulose membrane (Whatman, GE life technologies). Membranes were blocked with TBST (50 mM Tris pH 7.6, 0.15 M NaCl, 0.1 Tween-20) supplemented with 2% fish gelatin (Sigma) for 1 hour at

Europe PMC Funders Author Manuscripts

Europe PMC Funders Author Manuscripts

RT with gentle shaking, then washed 3 times with TBST and incubated with primary detection for 1 hour at RT (either 1/7000 diluted chicken anti-Neu5Gc IgY or biotinylated lectins; Bio-SNA diluted to 0.4 μg/ml and Bio-MALII diluted to 4μg/ml, as described in the figures legends). Next, membranes were washed 3 times with TBST and incubated with secondary detection (HRP-donkey-anti-chicken IgY 0.16 μg/ml or HRP-Streptavidin 0.1 μg/ml, respectively) for 1 hour at RT. Membranes were developed using an enhanced chemiluminescence kit (ECL; Pierce).

Sialic acid specificity analysis by mild periodate oxidation treatment

Freshly prepared NGs were diluted in SDS sample buffer to 40 ng/μl and incubated at room temperature for 30 min. The samples were separated on 12% SDS-PAGE gels, followed by transfer onto nitrocellulose membrane (Whatman, GE life technologies). Membranes were washed 3 times with ice cold water, once with ice cold PBS pH 6.5 (8.7 mM NaH_2PO_4, 137 mM NaCl), then incubated for 30 minutes with 2 mM of periodate diluted in PBS 6.5 at RT while protected from light. Then the membranes were washed 6 times with water and further analyzed by Western blotting, as described above.

Sialic acid analysis by lectin ELISA

NGs were coated onto 96-well microtiter plates (Costar, Corning) in duplicates at 1 μg protein/well in 50 mM sodium carbonate-bicarbonate buffer, pH 9.5 and incubated for overnight at 4 °C. Wells were blocked for 1 hour at RT with blocking buffer (PBS pH 7.4 with 1% ovalbumin), then aspirated and incubated with diluted primary antibody (chicken anti-Neu5Gc IgY at 1/1000, biotinylated SNA or MAL-II at 1 μg/ml) at 100 μl/well in the same blocking buffer for two hours at RT. Plates were washed three times with PBST (PBS pH 7.4, 0.1% Tween-20) and then incubated for 1 hour at RT with HRP-conjugated secondary antibody (HRP-donkey-anti-chicken IgY 0.26 μg/ml or HRP-streptavidin 0.1 μg/ml, respectively) in PBS. After washing three times with PBST, wells were developed with 140 μl of *O*-phenylenediamine in 100 mM of citrate-PO_4 buffer, pH 5.5, and the reaction was stopped with 40 μl of H_2SO_4 (4 M). Absorbance was measured at 490 nm on SpectraMax M3 (Molecular Devices). Specific binding was defined by subtracting the background readings obtained with the secondary antibody only on coated wells.

Sialoglycan microarray fabrication

Arrays were printed as described.[45] Briefly, arrays were fabricated with NanoPrint LM-60 Microarray Printer (Arrayit, CA) on epoxide-derivatized slides (Corning) with 16 sub-array blocks on each slide. Glycans were distributed into one 384-well source plates with 4 replicate wells per sample and 8 μl per well (Version 1.0). Each glycan was prepared at 100 μM in an optimized print buffer (300 mM phosphate buffer, pH 8.4). To monitor printing quality, replicate wells of mouse IgG (Jackson ImmunoResearch, at 200, 100, 50, 25, 12.5, 6.25 ng/μl in PBS+10% glycerol) and AlexaFlour-555-Hydraside (Invitrogen, at 1 ng/μl in 178 mM phosphate buffer, pH 5.5) were used for each printing run. The arrays were printed with four SMP3 pins (5 μm tip, 0.25 μl sample channel, ~100 μm spot diameter; Arrayit, CA). Each block (sub-array) had 17 spots/row, 20 columns with spot-to-spot spacing of 225 μm. The humidity level in the arraying chamber was maintained at about 66% during printing. Printed slides were left on arrayer deck overnight, allowing humidity to drop to

Europe PMC Funders Author Manuscripts

Europe PMC Funders Author Manuscripts

ambient levels (40-45%). Next, slides were packed, vacuum-sealed and stored at RT in a desiccant chamber until further use. Slides were printed in one batch of 56 slides.

NGs stability analysis using microarray

Arrays were printed using NanoPrint LM-60 Microarray Printer (Arrayit, CA) on epoxidederivatized slides (Corning) with 16 sub-array blocks on each slide. Glycans and freshly prepared NGs diluted to 40 ng/μl in 187 mM Phosphate Buffer pH 8.4 were distributed into one 384-well source plates with 4 replicate wells per sample and 8 μl per well. In addition, in order to investigate the stability of NGs, samples (40 μl from each NG preparation) were frozen for 5 minutes in −80 °C, quickly thawed and diluted to 40 ng/μl. This cycle was repeated twice and the diluted samples were printed as well. Synthetic glycans were also printed and diluted to 100 μM in 300 mM phosphate buffer, pH 8.4. To monitor printing quality, AlexaFlour-555-Hydraside (Invitrogen, at 1 ng/μl in 178 mM phosphate buffer, pH 5.5) was used for each printing run. The arrays were printed using 4 SMP3 pin (5 μm tip, 0.25 μl sample channel, ~100μm spot diameter; Arrayit, CA). Each block (sub-array) had 16 rows and 10 columns with spot-to-spot spacing of 225 μm. The humidity level in the arraying chamber was maintained at about 70% during printing. Printed slides were left on arrayer deck over-night, allowing humidity to drop to ambient levels (40-45%). Next, slides were packed, vacuum-sealed and stored at RT in a desiccant chamber until further use. Slides were developed using antibodies and lectins as described below and in relevant figure legend.

Evaluating anti-NG response in immunized mice using microarray

Arrays were printed using NanoPrint LM-60 Microarray Printer (Arrayit, CA) on epoxidederivatized slides (Corning) with 16 sub-array blocks on each slide. NGs as well as synthetic glycans were distributed into one 384-well source plates with 4 replicate wells per sample and 8 μl per well. Each NGs samples were diluted in PBS pH 7.4 to 100 ng/μl and synthetic glycans at 100 μM in 300 mM phosphate buffer, pH 8.4. To monitor printing quality, mouse IgG (Jackson ImmunoResearch) at 40 ng/μl in PBS+10% glycerol and AlexaFlour-555-Hydraside (Invitrogen, at 1 ng/μl in 178 mM phosphate buffer, pH 5.5) were used for each printing run. The arrays were printed using one SMP3 pin (5 μm tip, 0.25 μl sample channel, ~100μm spot diameter; Arrayit, CA). Each block (sub-array) had 14 rows and 6 columns with spot-to-spot spacing of 225 μm. The humidity level in the arraying chamber was maintained at about 70% during printing. Printed slides were left on arrayer deck over-night, allowing humidity to drop to ambient levels (40-45%). Next, slides were packed, vacuumsealed and stored at RT in a desiccant chamber until further use. Slides were developed using antibodies and lectins as described below and in relevant figure legend.

Glycan microarray binding assay

Slides were developed and analyzed as previously described.[45] Slides were rehydrated with dH_2O and incubated for 30 min in a staining dish with 50 °C pre-warmed 0.05 M ethanolamine in 0.1 M of Tris-HCl, pH 9.0 to block the remaining reactive epoxy groups on the slide surface, then washed with 50 °C pre-warmed dH_2O. Slides were centrifuged at 200 × g for 3 min, then fitted with ProPlate™ Multi-Array 16-well slide module (Invitrogen) to divide into the 16 sub-arrays (blocks). Slides were washed with PBST (PBS pH 7.4, 0.1%

Europe PMC Funders Author Manuscripts

Europe PMC Funders Author Manuscripts

Tween-20), aspirated and blocked with 200 μl/sub-array of blocking buffer (PBS/OVA; PBS pH 7.4, 1% ovalbumin) for 1 hour at RT with gentle shaking. Next, the blocking solution was aspirated and 100 μl/ block of primary detection (1/100 mice sera, or 1/7000 chicken anti-Neu5Gc IgY, or Bio-SNA 20 ng/μl) diluted in PBS/OVA was added, then slides were incubated at RT with gentle shaking for 2 hours. Slides were washed three times with PBST then with PBS for 5 min/wash with shaking. Bound antibodies were detected by incubating with secondary detection (Cy3-goat-anti-mouse IgG 1.5 μg/ml, or Cy3-donkey-anti-chicken IgY 1.5 μg/ml, or Cy3-Streptavidin 1.2 μg/ml) diluted in PBS was added at 200 μl/block, then incubated at RT for 1 hour. Slides were washed three times with PBST, then with PBS for 5 min/wash followed by removal from ProPlate™ Multi-Array slide module which were immediately dipped in a staining dish with dH_2O and were incubated for 10 min with shaking followed by centrifugation at 200 × g for 5 min. Dry slides were vacuum-sealed and stored in dark until scanning.

Array slide processing

Processed slides were scanned and analyzed as described at 10 μm resolution with a Genepix 4000B microarray scanner (Molecular Devices) using 350 gain.[45] Images were analyzed by Genepix Pro 6.0 software (Molecular Devices). Spots were defined as circular features with a variable radius and local background subtraction was performed. Data were analyzed by Excel.

Optimizing cancer vaccine mouse immunization protocol.

All animal experiments were conducted according to the guidelines of the Tel-Aviv University Institutional Animal Care and Use Committee. 6-10 weeks old *Cmah*$^{-/-}$ mice were i.p. immunized with either NG^{pos} or NG^{neg}. NGs at 2 mg/ml protein concentration were mixed 1:1 (by volume) with Freud's complete adjuvant (FCA) or Freud's incomplete adjuvant (FIA) until emulsified, then 200 μl were injected intraperitoneally (i.p.; 200 μg NG/ mouse). In the first immunization protocol (B2W; n=10), FCA i.p. immunization at week 0 was followed by two or three boost immunizations with FIA at two-week intervals (weeks 2, 4, 6; Figure 3A). In the second immunization protocol (B1W; n=10), FCA i.p. immunization at week 0 was followed by two boost immunizations with FIA at one-week intervals (weeks 1, 2), followed by another boost at week 6 (Figure 3A). To evaluate the developed anti-Neu5Gc antibodies response and kinetics, mice were bled (facial vein) on a weekly basis, collecting tubes were incubated overnight at 4 °C, then centrifuged at 17,000 × g for 2 min and the serum was collected. Samples were stored at −80 °C until analyzed by glycan microarray assays.

To evaluate the significance of Freund's adjuvant for the development of IgG antibodies, mice were immunized according to B2W protocol with 200 μg of either NG^{pos} or NG^{neg} in FCA/FIA (n=7 per group) or NG^{pos} in PBS only (n=7). Serum was collected as described above, before the first injection and 2 weeks after the second boost (at week 6).

Evaluating cancer vaccine efficacy *in vivo*

MC38-GFP cells (murine colon adenocarcinoma cells stably expressing GFP)[81] were grown in culture (DMEM with high glucose, 10% FCS, 1% Glutamine, 1% penn-strep) to 80%

Europe PMC Funders Author Manuscripts

Europe PMC Funders Author Manuscripts

confluence, lifted with PBS/EDTA (10 mM EDTA in PBS without Ca^{+2}/Mg^{+2}) then centrifuged at 1500 × g for 5 min at 4 °C and resuspended in DPBS. On week 7.5 after cancer vaccine (NG^{pos}) or control immunization (NG^{neg}), with either B2W or B1W protocols, *Cmah*$^{-/-}$ mice were subcutaneously injected at the flank with 0.5 × 10^6 MC38-GFP cells/mouse in 150 μl DPBS. Tumors were palpable 5 days later, and were measured every other day using a digital caliper, then tumor volumes calculated [(height × length × width)/2]. To evaluate the effect of low levels anti-Neu5Gc antibodies on tumor progression, *Cmah*$^{-/-}$ mice were immunized with 200 μg of either cancer vaccine (NG^{pos}) or control immunization (NG^{neg}) using the B2W protocol with only 2 FIA boost immunizations (weeks 2 and 4), and one week later (week 5) mice were inoculated with 0.5 × 10^6 MC38-GFP cells/mouse, then monitored as described above.

Preparation of intra-tumoral IgG

Tumors from cancer vaccine or control treated mice were harvested on day 21, sliced to small pieces (~2 mm) and incubated in DMEM with collagenase type II (1 mg/ml) and DNAse-I (0.5mg/ml) at 37 °C for 30 minutes (total volume of 3.5 ml / sample). The suspension was centrifuged for 10 minutes at 400 × g and the supernatant were collected, then again centrifuged at 400 × g for 5 min. Resulting supernatants were transferred to 15 ml tubes, and 50 μl of pre-washed protein A Sepharose 4 Fast Flow beads (GE Healthcare) were added to each tube. Samples were incubated at 4 °C for 48 hours while mixing, then loaded on a polyprep column (BioRad), washed 3 times with PBS, and eluted with 0.5 ml 0.1 M Glycine, pH 2.5 into tubes containing 120 μl of Tris-HCl buffer (1 M, pH 9.0). Purified IgG antibodies were stored at 4 °C until analyzed by glycan microarray assays.

Statistical analysis

One-way or Two-way analysis of variance (ANOVA) test for multiple comparison, or t-test, were performed using Graphpad Prism software (version 6). The results were expressed as mean ± STD or SEM (as indicated in the figure legends).

Supplementary Material

Refer to Web version on PubMed Central for supplementary material.

Acknowledgments

This work was supported by the European Union H2020 Program grants (ERC-2016-STG-716220) (to V. Padler-Karavani). Gal-KO pigs were kindly obtained from D. Sachs, TBRC, Boston.

References

1. Lesterhuis WJ, Haanen JB, Punt CJ. Cancer Immunotherapy--revisited. Nat Rev Drug Discovery. 2011; 10:591–600. [PubMed: 21804596]
2. Pardoll D, Allison J. Cancer Immunotherapy: Breaking the Barriers to Harvest the Crop. Nat Med. 2004; 10:887–892. [PubMed: 15340404]
3. Chen DS, Mellman I. Oncology Meets Immunology: The Cancer-Immunity Cycle. Immunity. 2013; 39:1–10. [PubMed: 23890059]
4. Restifo NP, Dudley ME, Rosenberg SA. Adoptive Immunotherapy for Cancer: Harnessing the T Cell Response. Nat Rev Immunol. 2012; 12:269–281. [PubMed: 22437939]

Europe PMC Funders Author Manuscripts

5. Rosenberg SA, Restifo NP. Adoptive Cell Transfer as Personalized Immunotherapy for Human Cancer. Science. 2015; 348:62–68. [PubMed: 25838374]
6. Fesnak AD, June CH, Levine BL. Engineered T Cells: The Promise and Challenges of Cancer Immunotherapy. Nat Rev Cancer. 2016; 16:566–581. [PubMed: 27550819]
7. Farkona S, Diamandis EP, Blasutig IM. Cancer Immunotherapy: The Beginning of the End of Cancer. BMC Med. 2016; 14:73. [PubMed: 27151159]
8. Allison JP. Immune Checkpoint Blockade in Cancer Therapy: The 2015 Lasker-Debakey Clinical Medical Research Award. JAMA, J Am Med Assoc. 2015; 314:1113–1114.
9. Sharma P, Wagner K, Wolchok JD, Allison JP. Novel Cancer Immunotherapy Agents With Survival Benefit: Recent Successes and Next Steps. Nat Rev Cancer. 2011; 11:805–812. [PubMed: 22020206]
10. Hu Z, Ott PA, Wu CJ. Towards Personalized, Tumour-Specific, Therapeutic Vaccines for Cancer. Nat Rev Immunol. 2017; 18:168–182. [PubMed: 29226910]
11. Azvolinsky A. Cancer Vaccines: Always a Bridesmaid, Never a Bride. J Natl Cancer Inst. 2013; 105:248–249. [PubMed: 23369950]
12. Bol KF, Schreibelt G, Gerritsen WR, de Vries IJ, Figdor CG. Dendritic Cell-Based Immunotherapy: State of the Art and Beyond. Clin Cancer Res. 2016; 22:1897–1906. [PubMed: 27084743]
13. Handy CE, Antonarakis ES. Sipuleucel-T for the Treatment of Prostate Cancer: Novel Insights and Future Directions. Future Oncol. 2017; 14:907–917. [PubMed: 29260582]
14. Türeci Ö, Vormehr M, Diken M, Kreiter S, Huber C, Sahin U. Targeting the Heterogeneity of Cancer With Individualized Neoepitope Vaccines. Clin Cancer Res. 2016; 22:1885–1896. [PubMed: 27084742]
15. Whiteside TL, Demaria S, Rodriguez-Ruiz ME, Zarour HM, Melero I. Emerging Opportunities and Challenges in Cancer Immunotherapy. Clin Cancer Res. 2016; 22:1845–1855. [PubMed: 27084738]
16. Zimmermann S, Lepenies B. Glycans as Vaccine Antigens and Adjuvants: Immunological Considerations. Methods Mol Biol. 2015; 1331:11–26. [PubMed: 26169732]
17. Anish C, Schumann B, Pereira CL, Seeberger PH. Chemical Biology Approaches to Designing Defined Carbohydrate Vaccines. Chem Biol. 2014; 21:38–50. [PubMed: 24439205]
18. Lockhart S. Conjugate Vaccines. Expert Rev Vaccines. 2003; 2:633–648. [PubMed: 14711325]
19. Lindberg AA. Glycoprotein Conjugate Vaccines. Vaccine. 1999; 17(Suppl 2):S28–36. [PubMed: 10506406]
20. Huang YL, Wu CY. Carbohydrate-Based Vaccines: Challenges and Opportunities. Expert Rev Vaccines. 2010; 9:1257–1274. [PubMed: 21087106]
21. Zheng XJ, Yang F, Zheng M, Huo CX, Zhang Y, Ye XS. Improvement of the Immune Efficacy of Carbohydrate Vaccines By Chemical Modification on the GM3 Antigen. Org Biomol Chem. 2015; 13:6399–6406. [PubMed: 25982227]
22. Ragupathi G, Damani P, Srivastava G, Srivastava O, Sucheck SJ, Ichikawa Y, Livingston PO. Synthesis of Sialyl Lewis(a) (Sle (a), Ca19-9) and Construction of an Immunogenic Sle(a) Vaccine. Cancer Immunol Immunother. 2009; 58:1397–1405. [PubMed: 19190907]
23. Son HY, Apostolopoulos V, Kim CW. T/Tn Immunotherapy Avoiding Immune Deviation. Int J Immunopathol Pharmacol. 2016; 29:812–817. [PubMed: 27760846]
24. Brooks SA, Carter TM, Royle L, Harvey DJ, Fry SA, Kinch C, Dwek RA, Rudd PM. Altered Glycosylation of Proteins in Cancer: What is the Potential for New Anti-Tumour Strategies. Anticancer Agents Med Chem. 2008; 8:2–21. [PubMed: 18220502]
25. Dube DH, Bertozzi CR. Glycans in Cancer and Inflammation--potential for Therapeutics and Diagnostics. Nat Rev Drug Discovery. 2005; 4:477–488. [PubMed: 15931257]
26. Kobata A, Amano J. Altered Glycosylation of Proteins Produced By Malignant Cells, and Application for the Diagnosis and Immunotherapy of Tumours. Immunol Cell Biol. 2005; 83:429–439. [PubMed: 16033539]
27. Kim YJ, Varki A. Perspectives on the Significance of Altered Glycosylation of Glycoproteins in Cancer. Glycoconj J. 1997; 14:569–576. [PubMed: 9298689]

Europe PMC Funders Author Manuscripts

28. Padler-Karavani V. Aiming At the Sweet Side of Cancer: Aberrant Glycosylation as Possible Target for Personalized-Medicine. Cancer Lett. 2014; 352:102–112. [PubMed: 24141190]
29. Angata T, Varki A. Chemical Diversity in the Sialic Acids and Related Alpha-Keto Acids: An Evolutionary Perspective. Chem Rev. 2002; 102:439–469. [PubMed: 11841250]
30. Chou HH, Takematsu H, Diaz S, Iber J, Nickerson E, Wright KL, Muchmore EA, Nelson DL, Warren ST, Varki A. A Mutation in Human Cmp-Sialic Acid Hydroxylase Occurred After the Homo-Pan Divergence. Proc Natl Acad Sci U S A. 1998; 95:11751–11756. [PubMed: 9751737]
31. Tangvoranuntakul P, Gagneux P, Diaz S, Bardor M, Varki N, Varki A, Muchmore E. Human Uptake and Incorporation of an Immunogenic Nonhuman Dietary Sialic Acid. Proc Natl Acad Sci U S A. 2003; 100:12045–12050. [PubMed: 14523234]
32. Bardor M, Nguyen DH, Diaz S, Varki A. Mechanism of Uptake and Incorporation of the Non-Human Sialic Acid N-Glycolylneuraminic Acid Into Human Cells. J Biol Chem. 2005; 280:4228–4237. [PubMed: 15557321]
33. Padler-Karavani V, Yu H, Cao H, Chokhawala H, Karp F, Varki N, Chen X, Varki A. Diversity in Specificity, Abundance, and Composition of Anti-Neu5Gc Antibodies in Normal Humans: Potential Implications for Disease. Glycobiology. 2008; 18:818–830. [PubMed: 18669916]
34. Padler-Karavani V, Hurtado-Ziola N, Pu M, Yu H, Huang S, Muthana S, Chokhawala HA, Cao H, Secrest P, Friedmann-Morvinski D, Singer O, et al. Human Xeno-Autoantibodies Against a Non-Human Sialic Acid Serve as Novel Serum Biomarkers and Immunotherapeutics in Cancer. Cancer Res. 2011; 71:3352–3363. [PubMed: 21505105]
35. Pearce OM, Laubli H, Verhagen A, Secrest P, Zhang J, Varki NM, Crocker PR, Bui JD, Varki A. Inverse Hormesis of Cancer Growth Mediated By Narrow Ranges of Tumor-Directed Antibodies. Proc Natl Acad Sci U S A. 2014; 111:5998–6003. [PubMed: 24711415]
36. Fang RH, Jiang Y, Fang JC, Zhang L. Cell Membrane-Derived Nanomaterials for Biomedical Applications. Biomaterials. 2017; 128:69–83. [PubMed: 28292726]
37. Su J, Sun H, Meng Q, Zhang P, Yin Q, Li Y. Enhanced Blood Suspensibility and Laser-Activated Tumor-Specific Drug Release of Theranostic Mesoporous Silica Nanoparticles By Functionalizing With Erythrocyte Membranes. Theranostics. 2017; 7:523–537. [PubMed: 28255347]
38. Luk BT, Fang RH, Hu CM, Copp JA, Thamphiwatana S, Dehaini D, Gao W, Zhang K, Li S, Zhang L. Safe and Immunocompatible Nanocarriers Cloaked in RBC Membranes for Drug Delivery to Treat Solid Tumors. Theranostics. 2016; 6:1004–1011. [PubMed: 27217833]
39. Villa CH, Pan DC, Zaitsev S, Cines DB, Siegel DL, Muzykantov VR. Delivery of Drugs Bound to Erythrocytes: New Avenues for an Old Intravascular Carrier. Ther Delivery. 2015; 6:795–826.
40. Steck TL. The Organization of Proteins in the Human Red Blood Cell Membrane. A Review. J Cell Biol. 1974; 62:1–19. [PubMed: 4600883]
41. Ganguly K, Murciano JC, Westrick R, Leferovich J, Cines DB, Muzykantov VR. The Glycocalyx Protects Erythrocyte-Bound Tissue-Type Plasminogen Activator From Enzymatic Inhibition. J Pharmacol Exp Ther. 2007; 321:158–164. [PubMed: 17215448]
42. Galili U. Discovery of the Natural Anti-Gal Antibody and Its Past and Future Relevance to Medicine. Xenotransplantation. 2013; 20:138–147. [PubMed: 23577774]
43. Naso F, Stefanelli U, Buratto E, Lazzari G, Perota A, Galli C, Gandaglia A. Alpha-Gal Inactivated Heart Valve Bioprostheses Exhibit an Anti-Calcification Propensity Similar to Knockout Tissues. Tissue Eng, Part A. 2017; 23:1181–1195. [PubMed: 29053434]
44. Salama A, Mosser M, Lévêque X, Perota A, Judor JP, Danna C, Pogu S, Mouré A, Jégou D, Gaide N, Abadie J, et al. Neu5Gc and α1-3 Gal Xenoantigen Knockout Does Not Affect Glycemia Homeostasis and Insulin Secretion in Pigs. Diabetes. 2017; 66:987–993. [PubMed: 28082457]
45. Leviatan Ben-Arye S, Yu H, Chen X, Padler-Karavani V. Profiling Anti-Neu5Gc IgG in Human Sera With a Sialoglycan Microarray Assay. J Visualized Exp. 2017; 125
46. Diaz SL, Padler-Karavani V, Ghaderi D, Hurtado-Ziol N, Yu H, Chen X, Brinkman-Van der Linden EC, Varki A, Varki NM. Sensitive and Specific Detection of the Non-Human Sialic Acid N-Glycolylneuraminic Acid in Human Tissues and Biotherapeutic Products. PLoS ONE. 2009; 4:e4241. [PubMed: 19156207]
47. Padler-Karavani V, Song X, Yu H, Hurtado-Ziola N, Huang S, Muthana S, Chokhawala HA, Cheng J, Verhagen A, Langereis MA, Kleene R, et al. Cross-Comparison of Protein Recognition of Sialic

Europe PMC Funders Author Manuscripts

Acid Diversity on Two Novel Sialoglycan Microarrays. J Biol Chem. 2012; 287:22593–22608. [PubMed: 22549775]

48. Siegrist C-A. Vaccine Immunology. Vaccines. 2008; 5:17–36.
49. Schunk MK, Macallum GE. Applications and Optimization of Immunization Procedures. ILAR J. 2005; 46:241–257. [PubMed: 15953832]
50. Pearce OM, Laubli H, Bui J, Varki A. Hormesis in Cancer Immunology: Does the Quantity of an Immune Reactant Matter? Oncoimmunology. 2014; 3:e29312. [PubMed: 25083340]
51. Okerblom J, Varki A. Biochemical, Cellular, Physiological, and Pathological Consequences of Human Loss of N-Glycolylneuraminic Acid. Chembiochem. 2017; 18:1155–1171. [PubMed: 28423240]
52. Hedlund M, Padler-Karavani V, Varki NM, Varki A. Evidence for a Human-Specific Mechanism for Diet and Antibody-Mediated Inflammation in Carcinoma Progression. Proc Natl Acad Sci U S A. 2008; 105:18936–18941. [PubMed: 19017806]
53. Samraj AN, Pearce OM, Läubli H, Crittenden AN, Bergfeld AK, Banda K, Gregg CJ, Bingman AE, Secrest P, Diaz SL, Varki NM, et al. A Red Meat-Derived Glycan Promotes Inflammation and Cancer Progression. Proc Natl Acad Sci U S A. 2015; 112:542–547. [PubMed: 25548184]
54. Samraj AN, Bertrand KA, Luben R, Khedri Z, Yu H, Nguyen D, Gregg CJ, Diaz SL, Sawyer S, Chen X, Eliassen H, et al. Polyclonal Human Antibodies Against Glycans Bearing Red Meat-Derived Non-Human Sialic Acid N-Glycolylneuraminic Acid Are Stable, Reproducible, Complex and Vary Between Individuals: Total Antibody Levels Are Associated With Colorectal Cancer Risk. PLoS One. 2018; 13:e0197464. [PubMed: 29912879]
55. Amon R, Ben-Arye SL, Engler L, Yu H, Lim N, Berre LL, Harris KM, Ehlers MR, Gitelman SE, Chen X, Soulillou JP, et al. Glycan Microarray Reveal Induced Iggs Repertoire Shift Against a Dietary Carbohydrate in Response to Rabbit Anti-Human Thymocyte Therapy. Oncotarget. 2017; 8:112236–112244. [PubMed: 29348821]
56. Yin J, Hashimoto A, Izawa M, Miyazaki K, Chen GY, Takematsu H, Kozutsumi Y, Suzuki A, Furuhata K, Cheng FL, Lin CH, et al. Hypoxic Culture Induces Expression of Sialin, a Sialic Acid Transporter, and Cancer-Associated Gangliosides Containing Non-Human Sialic Acid on Human Cancer Cells. Cancer Res. 2006; 66:2937–2945. [PubMed: 16540641]
57. Scott AM, Wolchok JD, Old LJ. Antibody Therapy of Cancer. Nat Rev Cancer. 2012; 12:278–287. [PubMed: 22437872]
58. Scott AM, Allison JP, Wolchok JD. Monoclonal Antibodies in Cancer Therapy. Cancer Immunity. 2012; 12:14. [PubMed: 22896759]
59. Poland GA, Ovsyannikova IG, Jacobson RM, Smith DI. Heterogeneity in Vaccine Immune Response: The Role of Immunogenetics and the Emerging Field of Vaccinomics. Clin Pharmacol Ther. 2007; 82:653–664. [PubMed: 17971814]
60. Antia A, Ahmed H, Handel A, Carlson NE, Amanna IJ, Antia R, Slifka M. Heterogeneity and Longevity of Antibody Memory to Viruses and Vaccines. PLoS Biol. 2018; 16:e2006601. [PubMed: 30096134]
61. Ye Z, Qian Q, Jin H, Qian Q. Cancer Vaccine: Learning Lessons From Immune Checkpoint Inhibitors. J Cancer. 2018; 9:263–268. [PubMed: 29344272]
62. Lollini PL, Cavallo F, Nanni P, Forni G. Vaccines for Tumour Prevention. Nat Rev Cancer. 2006; 6:204–216. [PubMed: 16498443]
63. Bethune MT, Joglekar AV. Personalized T Cell-Mediated Cancer Immunotherapy: Progress and Challenges. Curr Opin Biotechnol. 2017; 48:142–152. [PubMed: 28494274]
64. Finn OJ. Human Tumor Antigens Yesterday, Today, and Tomorrow. Cancer Immunol Res. 2017; 5:347–354. [PubMed: 28465452]
65. Padler-Karavani V. Glycan Microarray Reveal the Sweet Side of Cancer Vaccines. Cell Chem Biol. 2016; 23:1446–1447. [PubMed: 28009977]
66. Amon R, Reuven EM, Leviatan Ben-Arye S, Padler-Karavani V. Glycans in Immune Recognition and Response. Carbohydr Res. 2014; 389:115–122. [PubMed: 24680512]
67. Samraj AN, Läubli H, Varki N, Varki A. Involvement of a Non-Human Sialic Acid in Human Cancer. Front Oncol. 2014; 4:33. [PubMed: 24600589]

Europe PMC Funders Author Manuscripts

68. Magnani M, Chiarantini L, Vittoria E, Mancini U, Rossi L, Fazi A. Red Blood Cells as an Antigen-Delivery System. Biotechnol Appl Biochem. 1992; 16:188–194. [PubMed: 1457052]
69. Banz A, Cremel M, Mouvant A, Guerin N, Horand F, Godfrin Y. Tumor Growth Control Using Red Blood Cells as the Antigen Delivery System and Poly(I:C). J Immunother. 2012; 35:409–417. [PubMed: 22576346]
70. Banz A, Cremel M, Rembert A, Godfrin Y. *In Situ* Targeting of Dendritic Cells By Antigen-Loaded Red Blood Cells: A Novel Approach to Cancer Immunotherapy. Vaccine. 2010; 28:2965–2972. [PubMed: 20188177]
71. Springer GF. Immunoreactive T and Tn Epitopes in Cancer Diagnosis, Prognosis, and Immunotherapy. J Mol Med (Berl). 1997; 75:594–602. [PubMed: 9297627]
72. Muzykantov VR. Drug Delivery By Red Blood Cells: Vascular Carriers Designed By Mother Nature. Expert Opin Drug Delivery. 2010; 7:403–427.
73. Rao L, Bu LL, Xu JH, Cai B, Yu GT, Yu X, He Z, Huang Q, Li A, Guo SS, Zhang XZ, et al. Red Blood Cell Membrane as a Biomimetic Nanocoating for Prolonged Circulation Time and Reduced Accelerated Blood Clearance. Small. 2015; 11:6225–6236. [PubMed: 26488923]
74. Xia L, Schrump DS, Gildersleeve JC. Whole-Cell Cancer Vaccines Induce Large Antibody Responses to Carbohydrates and Glycoproteins. Cell Chem Biol. 2016; 23:1515–1525. [PubMed: 27889407]
75. Schumann B, Reppe K, Kaplonek P, Wahlbrink A, Anish C, Witzenrath M, Pereira CL, Seeberger PH. Development of an Efficacious, Semisynthetic Glycoconjugate Vaccine Candidate Against. ACS Cent Sci. 2018; 4:357–361. [PubMed: 29632881]
76. Geissner A, Seeberger PH. Glycan Arrays: From Basic Biochemical Research to Bioanalytical and Biomedical Applications. Annu Rev Anal Chem (Palo Alto Calif). 2016; 9:223–247. [PubMed: 27306309]
77. Pappalardo F, Pennisi M, Castiglione F, Motta S. Vaccine Protocols Optimization: *In Silico* Experiences. Biotechnol Adv. 2010; 28:82–93. [PubMed: 19833190]
78. Zahm CD, Colluru VT, McNeel DG. Vaccination With High-Affinity Epitopes Impairs Antitumor Efficacy By Increasing PD-1 Expression on CD8. Cancer Immunol Res. 2017; 5:630–641. [PubMed: 28634215]
79. Butterfield LH. Cancer Vaccines. BMJ. 2015; 350:h988. [PubMed: 25904595]
80. Zeng M, Nourishirazi E, Guinet E, Nouri-Shirazi M. The Genetic Background Influences the Cellular and Humoral Immune Responses to Vaccines. Clin Exp Immunol. 2016; 186:190–204. [PubMed: 27393001]
81. Borsig L, Wong R, Hynes RO, Varki NM, Varki A. Synergistic Effects of L- and P-Selectin in Facilitating Tumor Metastasis Can Involve Non-Mucin Ligands and Implicate Leukocytes as Enhancers of Metastasis. Proc Natl Acad Sci U S A. 2002; 99:2193–2198. [PubMed: 11854515]

Europe PMC Funders Author Manuscripts

Europe PMC Funders Author Manuscripts

Europe PMC Funders Author Manuscripts

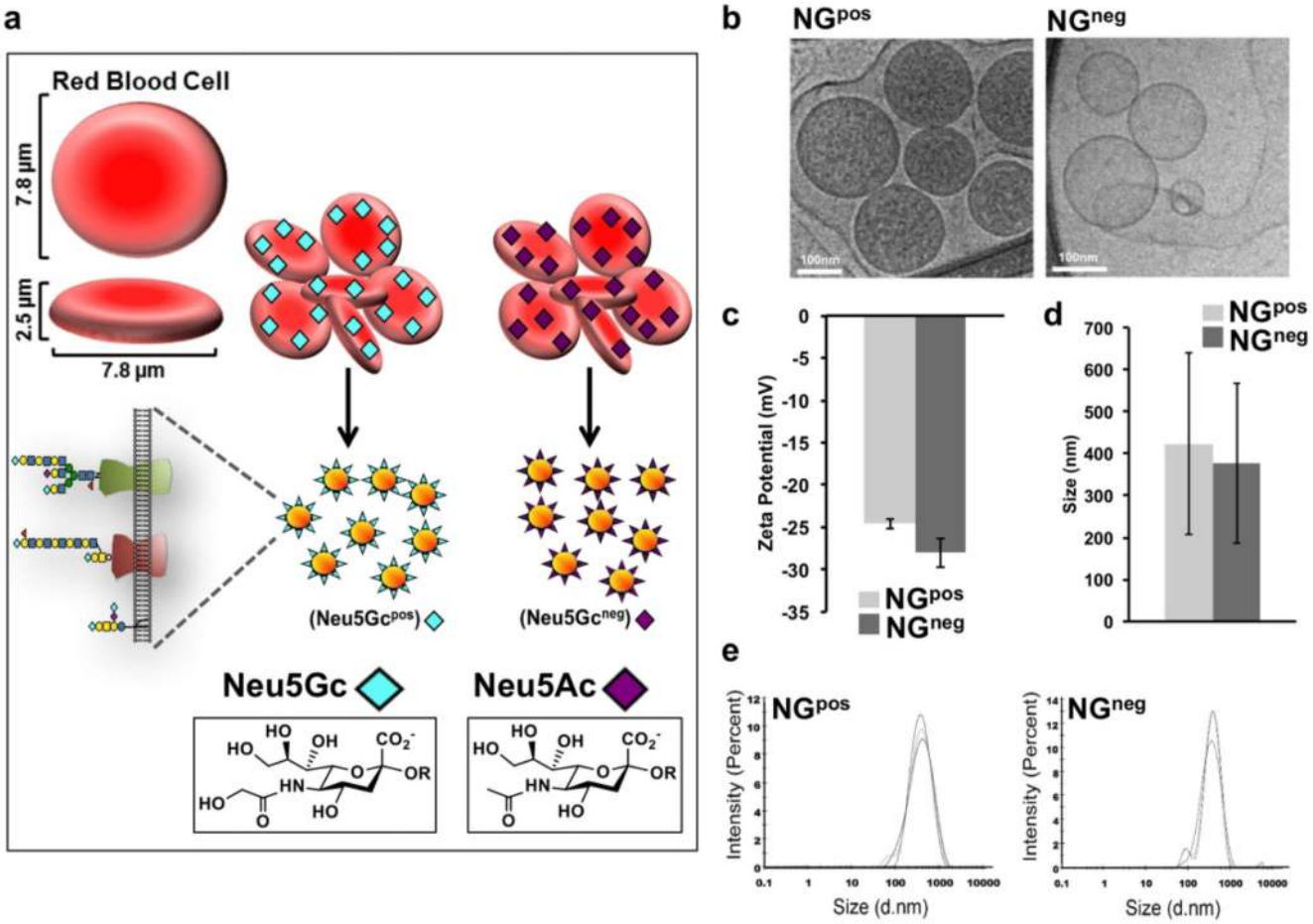

Figure 1.

Physiochemical characterization of porcine-derived nano-ghosts (NGs). (a) Schematic representation of red blood cells (RBCs) and NGs prepared from RBCs of two porcine strains that express various Sia-containing glycoproteins with either terminal Neu5Gc (αGal-deficient strain; NG^{pos}) or terminal Neu5Ac (Neu5Gc- and αGal-deficient strain; NG^{neg}). (b) Transmission electron micrograph (TEM) analysis of NG^{pos} and NG^{neg}. Freshly prepared NGs were applied onto a plasma etched carbon grid in CryoPlunge™ 3 unit (Gatan Instruments) employing a double blot technique for 2 s, then plunged into liquid ethane and transferred under liquid nitrogen to cryo-TEM (FEI; Tecnai G2). Images were captured using a DigitalMicrograph software (Gatan) (representative of two independent experiments). (c) Zeta potential of freshly prepared NGs was measured. (d-e) Size of freshly prepared NGs was measured. NGs were diluted to 20 µg protein/ml (in ddH_2O for Zeta potential, or PBS pH 7.4 for size) and measured in a Malvern Nano ZS Zetasizer (Each experimental result is an average of at least three independent measurements).

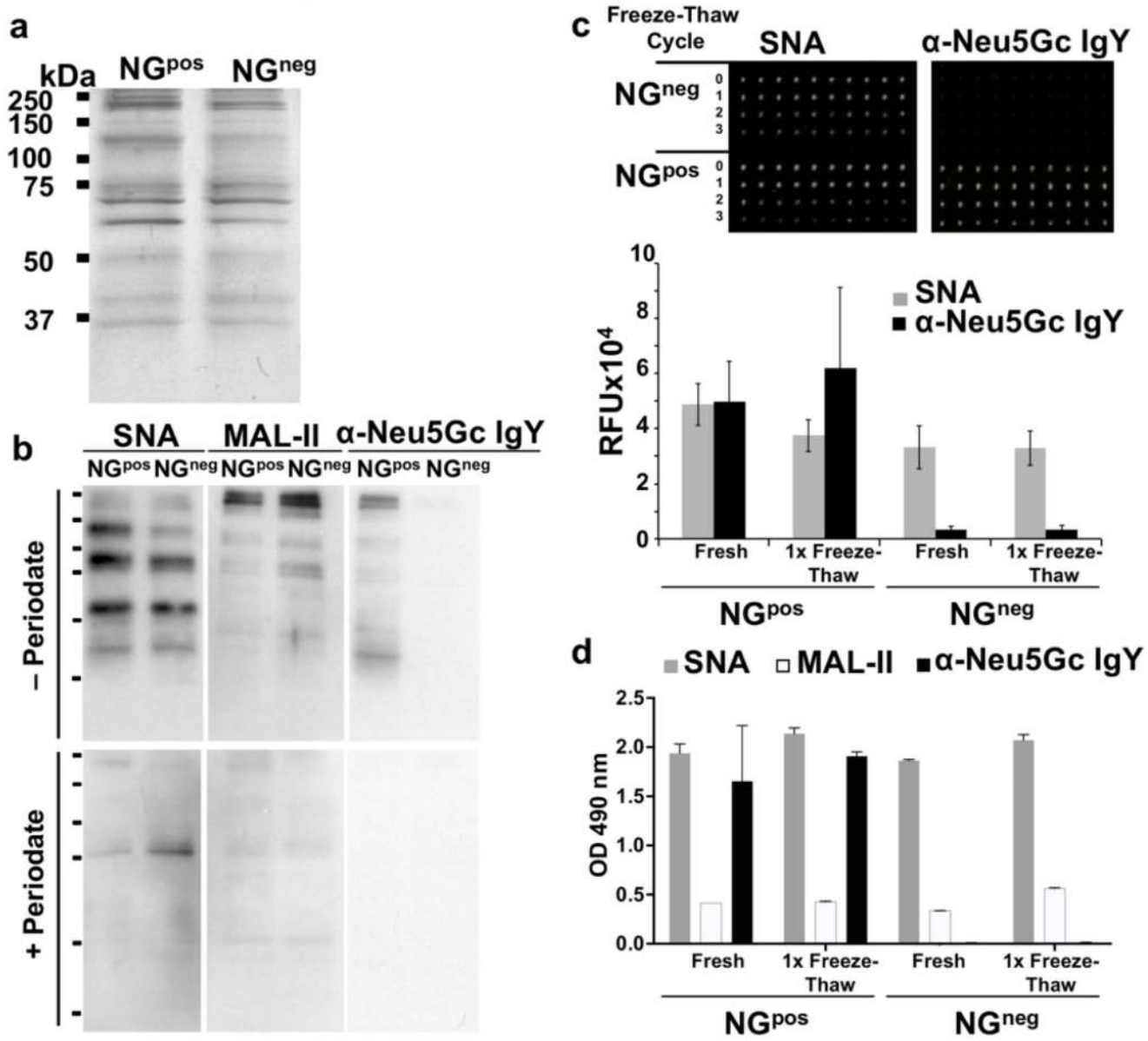

Figure 2.

Biochemical characterization of NG^{pos} and NG^{neg}. NGs were diluted in sample buffer to 40 μg protein/ml, loaded 10 μl/lane, then separated on 12% SDS-PAGE gel. (a) Silver staining of freshly prepared NGs revealed similar protein content in both NG^{pos} and NG^{neg}. (b) Sialic acid content of NGs was analyzed by Western blot with the biotinylated lectins Bio-SNA (binds Siaα2–6-linked) and Bio-MAL-II (binds Siaα2–3-linked), detected by HRP-streptavidin; and chicken anti-Neu5Gc IgY detected by HRP-donkey-anti-chicken IgY. Specificity was analyzed by pre-treatment of the blot with mild periodate oxidation (bottom panel; + Periodate) that truncates Sia side chain (carbons C-8 and C-9), leading to loss of Sia-specific binding compared to mock treatment (top panel; – Periodate) (representative of two independent experiments). (c) NGs stability after freeze-thaw was assessed by Sia

Europe PMC Funders Author Manuscripts
Europe PMC Funders Author Manuscripts

surface expression analyzed by microarray. (d) NGs stability was also measured by ELISA. Fresh and freeze-thawed NGs were printed with NanoPrint arrayer at 40 μg protein/ml on epoxide-coated glass slide (10 replicates per sample), or coated at 1 μg protein/well to 96-well plate in triplicates for ELISA. Samples were then analyzed as indicated with Bio-SNA, Bio-MAL-II and anti-Neu5Gc IgY, respectively detected by streptavidin and donkey-anti-chicken IgY [HRP-conjugated (c) or Cy3-conjugated (d)], demonstrating right-side-out orientation and stability after one freeze-thaw cycle (representative of at least two independent experiments; mean ± SD).

Europe PMC Funders Author Manuscripts

Europe PMC Funders Author Manuscripts

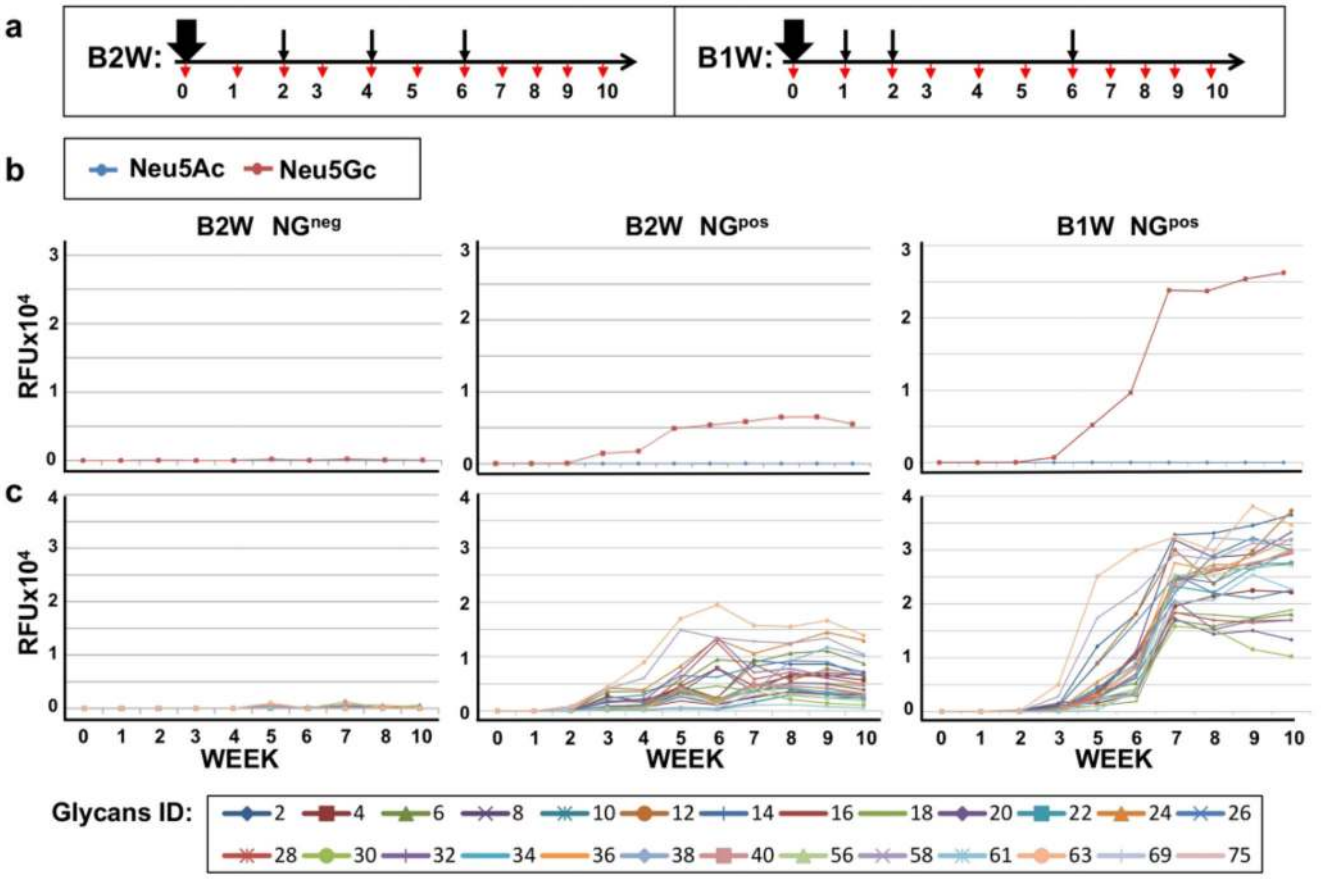

Figure 3.

Optimization of vaccination regimen. (a) Schematic representation of the immunization regimen. *Cmah*$^{-/-}$ mice were immunized intraperitoneally (i.p.) with 200 μl of 1 μg/μl NG^{neg} or NG^{pos} (n=7 per group) emulsified in Freud's Complete Adjuvant (FCA; thick black arrow), then boosted three times with NGs in Freud's Incomplete Adjuvant (FIA; thin black arrows) at initial one or two weeks intervals, as indicated (B1W, B2W, respectively). Mouse serum was sampled on day 0 then weekly (red arrows). Sera samples were then analyzed by sialoglycan microarrays containing diverse sialoglycans, detected with Cy3-labeled anti-mouse IgG. (b) The average IgG response of the 7 mice in each group is presented as average response against mono-sialylated Neu5Gc-glycans (n=24; red) and Neu5Ac-glycans (n=24; blue). (c) Array response against the 24 individual Neu5Gc-glycans (colored lines; full list of glycans in supplementary Table 1).

Europe PMC Funders Author Manuscripts
Europe PMC Funders Author Manuscripts

Europe PMC Funders Author Manuscripts

Europe PMC Funders Author Manuscripts

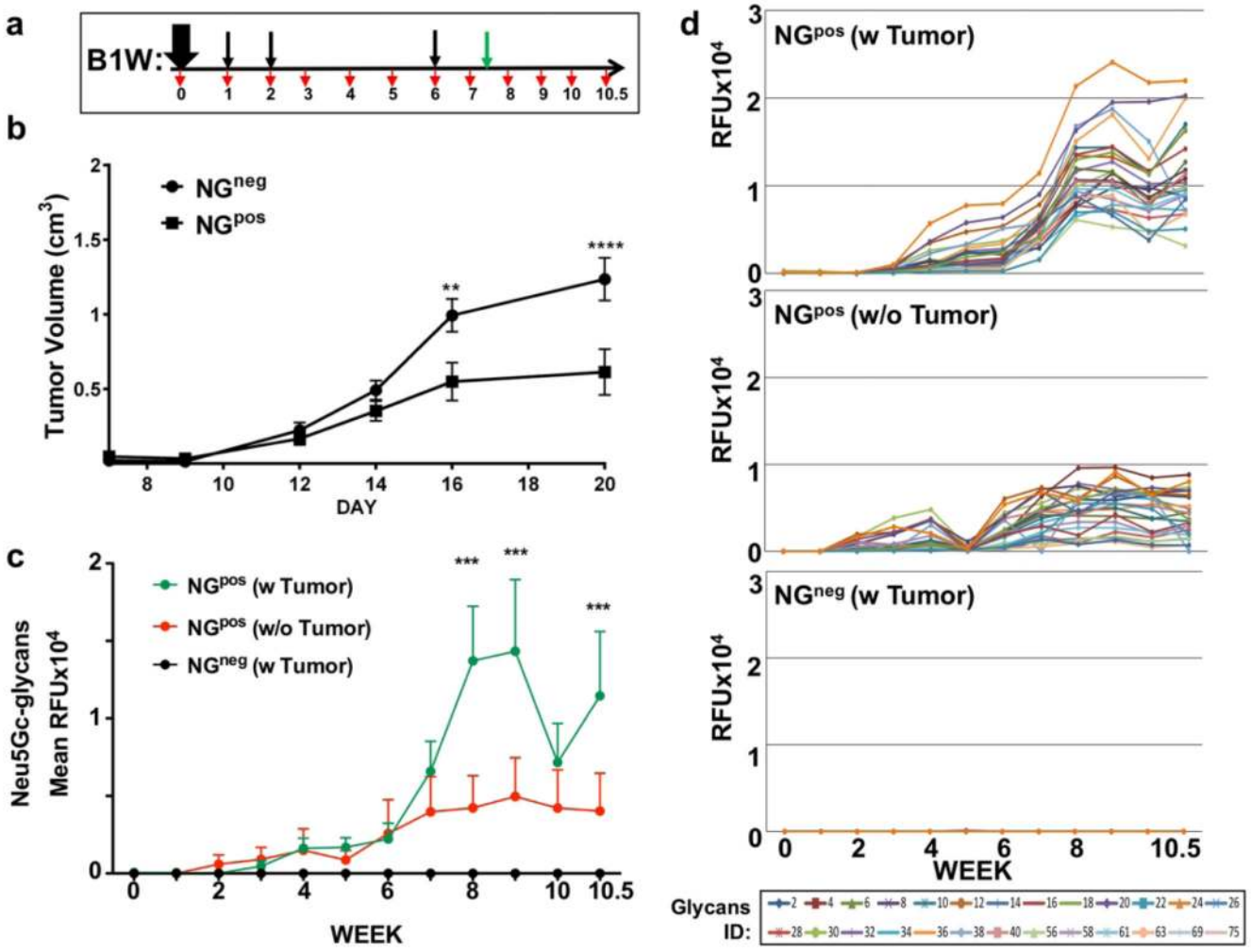

Figure 4.

Cancer vaccine inhibit tumor growth *in vivo*. (a) Schematic representation of experimental design. *Cmah*$^{-/-}$ mice were immunized intraperitoneally (i.p.) with NG^{neg} or NG^{pos} (n=10 per group) in the optimized B1W regimen. Mouse serum was sampled on day 0 then weekly (red arrows). On week 7.5, 0.5 × 10^6 MC38-GFP cells were inoculated subcutaneously (green arrow). (b) Tumor volumes were monitored every other day showing inhibition of tumor growth in the NG^{pos} vaccine-treated group (mean ±SEM; One-Way ANOVA with Bonferroni posttests, ** p<0.01, *** p<0.001; in NG^{pos} group, two mice became necrotic on week 10 and were excluded from analysis). (c) Sera samples were then analyzed by sialoglycan microarrays containing diverse sialoglycans, detected with Cy3- labeled anti-mouse IgG. Each line represents the average response of 10 mice per group against all Neu5Gc-glycans. (d) Array response agaisns the 24 individual Neu5Gc-glycans (colored lines).

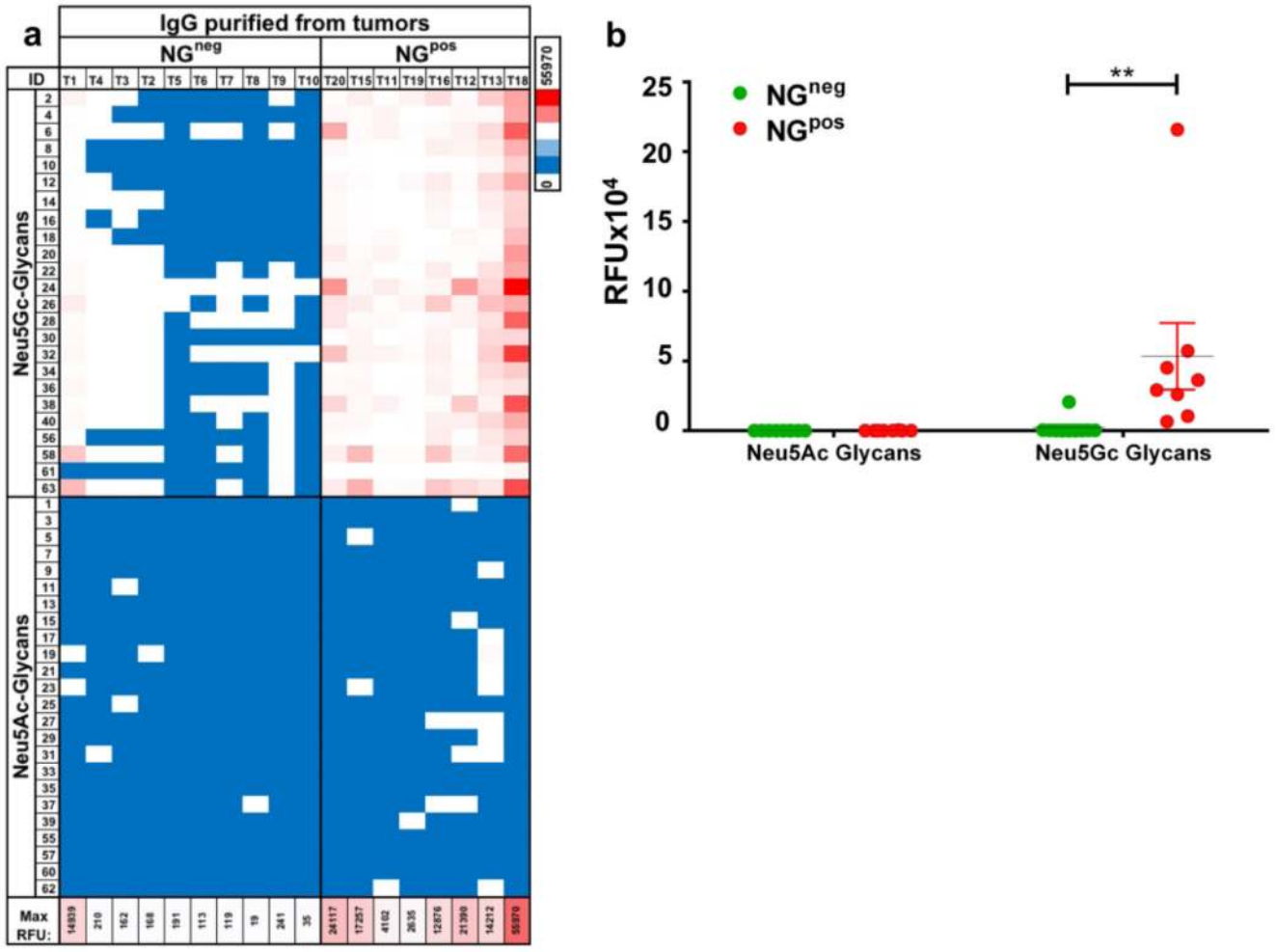

Figure 5.

Intra-tumoral IgG recognize Neu5Gc-glycans. (a) Tumors were harvested from vaccine or control immunized mice (NG^{pos} or NG^{neg}, respectively), minced and then IgG antibodies were purified with Protein-A. 20 ng/μl of intra-tumoral purified IgG antibodies were analyzed on sialoglycan microarrays, then detected by Cy3-anti-mouse IgG. Results are presented as heat map of IgG reactivity in relative fluorescent units (RFU), per glycan per mouse, against the collection of Neu5Gc-glycans or Neu5Ac-glycans (Blue-white-red scale represent 0-50-100 percentiles). (b) Average IgG response of individual mice against Neu5Gc-glycan or Neu5Ac-glycans on microarray (Two-Way ANOVA with Bonferroni posttests, ** $p<0.01$).

Europe PMC Funders Author Manuscripts
Europe PMC Funders Author Manuscripts

Europe PMC Funders Author Manuscripts

Europe PMC Funders Author Manuscripts

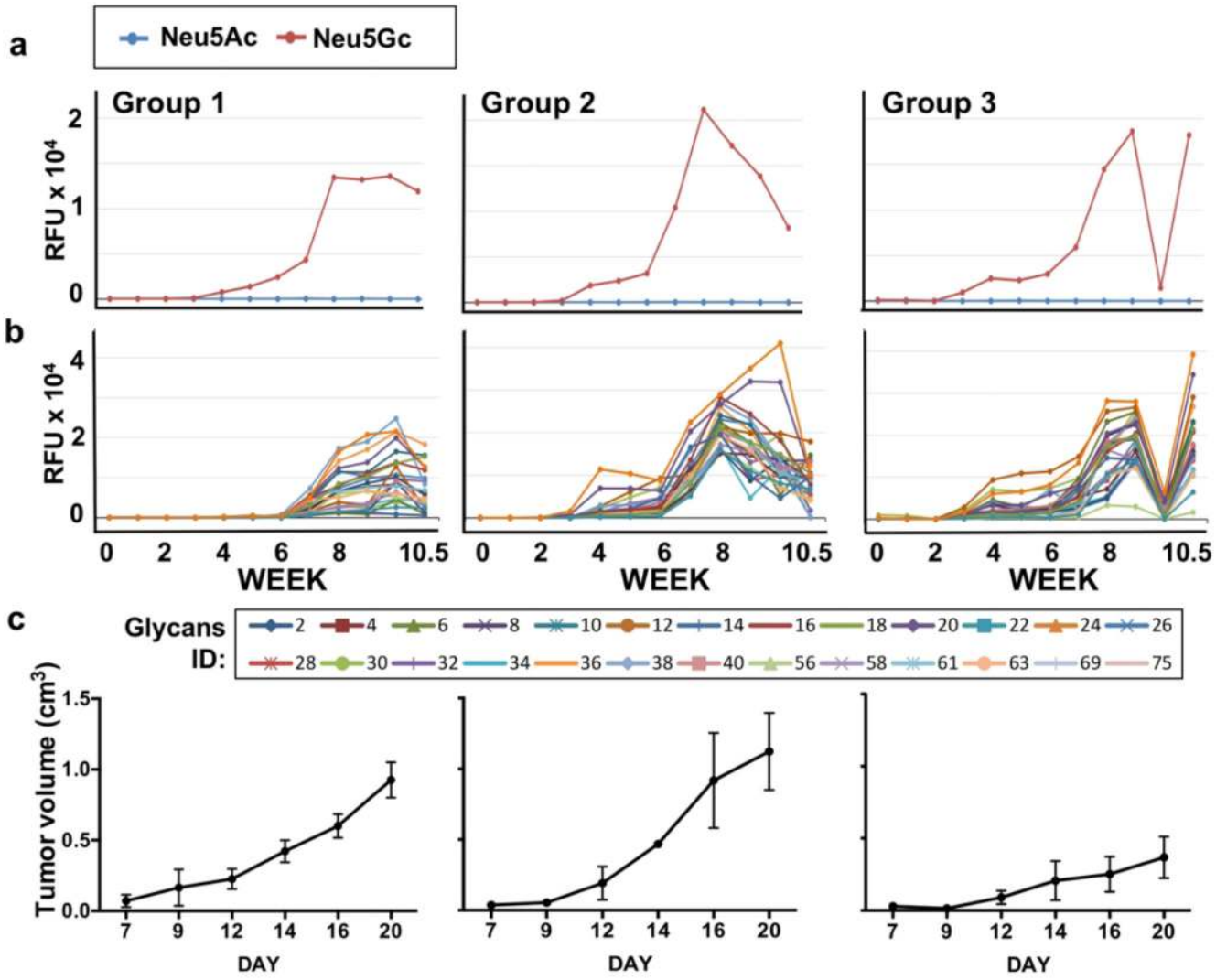

Figure 6.

Kinetics of anti-Neu5Gc IgG response and tumor growth in vaccine treated mice. Glycan microarray analysis and tumor growth kinetics in mice of the vaccine treated group that was inoculated with tumors (NG^{pos} w/Tumor; B1W; Figure 4). These mice were divided into three group types, according to their antibodies and tumor volume kinetic of response. (a) Average IgG response against all Neu5Gc-glycans and all Neu5Ac-glycans, per group. (b) Average IgG response against individual Neu5Gc-glycans, per group. (c) Average of tumor growth kinetics, per group.